Geodesy and Geodynamics xxx (xxxx) xxx

Contents lists available at ScienceDirect

Geodesy and Geodynamics

journal homepage: http://www.keaipublishing.com/geog

Contribution of the BDS to availability and reliability improvement: A case study of dam surface displacement monitoring in China

Shanqi Huang [a, b, c, *], Junping Chen [c], Hu Wang [d, e]

[a] College of Civil Engineering and Architecture, Guangxi University, Nanning, China
[b] Engineering Disaster Prevention and Structural Safety (Key Laboratory of Education Ministry, Key Laboratory of Guangxi), Guangxi University, Nanning, China
[c] Shanghai Astronomical Observatory, China Academy of Sciences, Shanghai, China
[d] Chinese Academy of Surveying & Mapping, Beijing, China
[e] School of Geodesy and Geomatics, Wuhan University, Wuhan, China

ARTICLE INFO

Article history:
Received 14 July 2018
Accepted 27 February 2019
Available online xxx

Keywords:
Dam surface monitoring
BDS
Availability
Reliability

ABSTRACT

The GPS-only system is limited in dam surface monitoring because of its low availability and reliability due to the visible satellites are not enough. This dilemma is expected to be solved through incorporating the China's BeiDou System (BDS). This contribution will quantitatively analyse the availability and reliability improvements from DBS in different shielding situations of dams. The analysis is conducted through simulating a dam obstruction with different size, azimuth and distance to receiver. The similar experiments are simulated in the area across China in order to explore these contributions in different locations. Quantitative analysis results derive conclusions: (1) In most areas, the availability improved from 50% of GPS-only to 95% of BDS + GPS when most of the GEO/IGSO satellites are not blocked, and to 70% even when most of GEO/IGSO satellites are blocked. (2) The average MDBs can be reduced by half when most of the GEO/IGSO satellites are not blocked, and by 10% even when most of GEO/IGSO satellites are blocked.

1. Introduction

The GPS-only deformation monitoring system is hard to work when the receiver is shielded by huge obstructions, because of limited visible satellites, low availability and reliability [1–3]. Dam surface monitoring is a typical high-shielding obstruction situation, especially the concrete dam with large obliquity. Because GPS-only deformation system can't work, dam surface displacement monitoring is typically worked with measuring robot, three-dimensional laser scanner [4,5] or terrestrial interferometric [6]. However, it is hard to achieve an all-weather and real-time monitoring result with these technologies. It is meaningful to find a scheme to make the GNSS receiver useful for dam surface monitoring. A feasible way is to employ a multi-constellation monitoring system. With development of Global Navigation Satellites System (GNSS), multi-constellation processing has been widely used. Generally, multi-constellation can effectively improve the geometric distribution of tracking satellites [7], and improve the availability of the monitoring system. Furthermore, modernized GPS and BDS provide triple-frequency observations (such as L5 of GPS and L3 of BDS). Multi-frequency observation can improve the reliability obviously [8,9]. Because of the characteristics of the BDS constellation, combining BDS with GPS can significantly increase the number of visible satellites in China. This is mainly thanks to the two types of geostationary satellites of BDS: geostationary Earth orbit(GEO) and inclined geosynchronous satellite orbit(IGSO). Therefore, the BDS + GPS deformation monitoring system will ameliorate the geometric limitation and improve the availability and reliability of

* Corresponding author. College of Civil Engineering and Architecture, Guangxi University, Nanning, China.
E-mail address: Shanqi_huang@163.com (S. Huang).

Peer review under responsibility of Institute of Seismology, China Earthquake Administration.

Production and Hosting by Elsevier on behalf of KeAi

https://doi.org/10.1016/j.geog.2019.02.001

positioning, particularly in the case of shielding by large obstructions.

This contribution will quantitatively analyse the availability and reliability improvements achieved by combing BDS with GPS for dam surface monitoring in different shielding situations. Availability is defined by the percentage of usable epochs for which the dilution of precision (DOP) is smaller than a given threshold; while reliability is reflected by the minimal detected bias (MDB) of the given observation models. To comprehensively evaluate the contributions of BDS to availability and reliability, some experiments are developed by simulating a dam obstruction with varying scenarios specified with different sizes, azimuths and distances to receiver. To further understand the contributions of BDS to deformation monitoring in different locations, similar experiments are processed in 2° × 2° grids over the whole area across China (latitude from 0° to N54° and longitude from E70° to E136°). The receive location and satellite ephemeris are the needed data in these simulations.

This contribution is organized as follow. In section 2, the mathematical models of GPS-only and BDS + GPS are presented, then the definition of availability and reliability are introduced. The simulation experiments and result analysis are shown in section 3. The conclusions are summarized in the section 4.

2. Observations model for analysis and index definition

In this section, we present the mathematical model for availability and reliability analysis, then explore the definition of analysis indexes. This contribution employs the double-difference (DD) processing method that is widely used in many kinds of deformation monitoring because of its simple model and fast processing speed.

In the following, the bold-lowercase letter means vectors, while bold-uppercase one matrix. $\boldsymbol{e}_n$ and $\boldsymbol{I}_n$ are the n-dimensions identify vector and matrix, respectively. $diag(\ldots)$ means a diagonal matrix with value in parentheses as diagonal elements. $blkdiag(\ldots)$ denotes a block diagonal matrix with value in parentheses as diagonal matrices. ⊗ denotes the Kronecker product.

2.1. Mathematical model for analysis

Let us start with the code and phase DD observation of f_{j^G} frequency for a single baseline (shorter than 5 km usually) in one epoch:

$$\begin{cases} E\left(\boldsymbol{p}_{j^G}\right) = \boldsymbol{M}^G\boldsymbol{x} + \mu_{j^G}\boldsymbol{\iota}^G \\ E\left(\boldsymbol{\varphi}_{j^G}\right) = \boldsymbol{M}^G\boldsymbol{x} - \mu_{j^G}\boldsymbol{\iota}^G + \lambda_{j^G}\boldsymbol{a}_{j^G} \end{cases} \tag{1}$$

where the superscript in each parameter means the satellite system: superscript 'G' denotes GPS, while 'C' denotes BDS; $\boldsymbol{p}_j$ and $\boldsymbol{\varphi}_j$ are the DD code and phase observations in meters, respectively; $\boldsymbol{x}$ is the between-receiver coordinate difference, with the design matrix $\boldsymbol{M}$; ι is the DD ionospheric delay with $\mu_j = f_1^2/f_j^2$ as its coefficient; $\mathbf{a}_j$ is the DD integer ambiguity, λ_j is the wavelength of this frequency. Assuming there are n tracked satellites and *1* is the reference satellite, then $\boldsymbol{p}_j = \begin{bmatrix} p_j^{12} & \cdots & p_j^{1n} \end{bmatrix}^T$; $\boldsymbol{\varphi}_j$, $\boldsymbol{M}$, ι and $\boldsymbol{a}_j$ have the same structure as $\boldsymbol{p}_j$. There is no need to consider the tropospheric delay if the baseline is short enough.

Assume there are k frequencies, combine observable of all frequencies together and increase the ionospheric delay constraint:

$$\begin{cases} E\left(\boldsymbol{y}^G\right) = \boldsymbol{A}^G\boldsymbol{x} + \boldsymbol{L}^G\boldsymbol{\iota}^G + \boldsymbol{N}^G\boldsymbol{a}^G \\ \iota_0^G\boldsymbol{e}_{n-1} = \boldsymbol{\iota}^G \text{ with } D\left(\boldsymbol{\iota}_0^G\right) = q_\iota^G\boldsymbol{I}_{n-1} \end{cases} \tag{2}$$

where $\boldsymbol{y} = \begin{bmatrix} \boldsymbol{p}^T & \boldsymbol{\varphi}^T \end{bmatrix}^T$, with $\boldsymbol{p} = \begin{bmatrix} \boldsymbol{p}_1^T & \cdots & \boldsymbol{p}_k^T \end{bmatrix}^T$ and $\boldsymbol{\varphi}$ has the same structure; $\boldsymbol{A} = \boldsymbol{e}_{2k} \otimes \boldsymbol{M}$, and $\boldsymbol{M}$ has the same structure as $\boldsymbol{p}$; $\boldsymbol{L} = (\boldsymbol{\Lambda} \otimes \bar{\boldsymbol{e}}_\iota \otimes \boldsymbol{I}_{n-1})/\lambda_1^2$ with $\boldsymbol{\Lambda} = \mathrm{diag}(f_1 \ \cdots \ f_k)$ and $\bar{\boldsymbol{e}}_\iota = \begin{bmatrix} -1 & 1 \end{bmatrix}^T$; $\boldsymbol{N} = \boldsymbol{\Lambda} \otimes \bar{\boldsymbol{e}}_a \otimes \boldsymbol{I}_{n-1}$ with $\bar{\boldsymbol{e}}_a = \begin{bmatrix} 0 & 1 \end{bmatrix}^T$, $\boldsymbol{a}$ has the same structure as $\boldsymbol{p}$. This model will estimate ionospheric delay every epoch with the additional constraint [9]. The $\boldsymbol{\iota}_0$ is usually given 0 for a baseline shorter than 20 km, while the q_ι 3 cm.

The model of BDS is similar to the GPS one. The final model combines the GPS and BDS models together:

$$\begin{cases} E(\boldsymbol{y}) = \boldsymbol{A}\boldsymbol{x} + \boldsymbol{L}\boldsymbol{\iota} + \boldsymbol{N}\boldsymbol{a} \\ \boldsymbol{\iota}_0 = \boldsymbol{\iota} \text{ with } D(\boldsymbol{\iota}_0) = \boldsymbol{Q}_\iota \end{cases} \tag{3}$$

where $\boldsymbol{y} = \begin{bmatrix} \boldsymbol{y}^G \\ \boldsymbol{y}^C \end{bmatrix}$, $\boldsymbol{A}$, $\boldsymbol{\iota}$, $\boldsymbol{\iota}_0$ and $\boldsymbol{a}$ have the same structure as it; $\boldsymbol{L} = \begin{bmatrix} \boldsymbol{L}^G & \\ & \boldsymbol{L}^C \end{bmatrix}$, and $\boldsymbol{N}$, $\boldsymbol{Q}_\iota$ have the same structure as $\boldsymbol{L}$.

The stochastic model is very important to the reliability analysis. Let us start with the variance matrix of single frequency DD observable of model (1) in terms of:

$$\begin{cases} \boldsymbol{Q}_{p_{j^G}} = \boldsymbol{D}\boldsymbol{Q}_{p_{j^G}}^0\boldsymbol{D}^T \\ \boldsymbol{Q}_{\phi_{j^G}} = \boldsymbol{D}\boldsymbol{Q}_{\phi_{j^G}}^0\boldsymbol{D}^T \end{cases} \tag{4}$$

where $\boldsymbol{Q}_{p_j}^0 = diag\left((\delta_{p_j}^1)^2 \ \cdots \ (\delta_{p_j}^n)^2 \right)$ is variance matrix of the j-th frequency zero difference (ZD) code observable with $\delta_{p_j}^i$ as it's uncertainty; $\boldsymbol{Q}_{\phi_j}^0$ is for phase observable, and has the similar structure as $\boldsymbol{Q}_{p_j}^0$; $\boldsymbol{D} = \begin{bmatrix} 1 & -1 \end{bmatrix} \otimes \begin{bmatrix} -\boldsymbol{e}_{n-1} & \boldsymbol{I}_{n-1} \end{bmatrix}$ is the DD mapping matrix. Then variance matrix of the GPS-only model(2) is $\boldsymbol{Q}_{\boldsymbol{y}^G}^0 = diag\left(\boldsymbol{Q}_{\boldsymbol{p}_{j^G}} \ \cdots \ \boldsymbol{Q}_{\boldsymbol{\varphi}_{j^G}} \right)$. The stochastic model of the first equation of the GPS + BDS model (3) can be denoted as:

$$\boldsymbol{Q}_{\mathbf{y}} = blkdiag\left(\boldsymbol{Q}_{\boldsymbol{y}^G} \quad \boldsymbol{Q}_{\boldsymbol{y}^C} \right) \tag{5}$$

2.2. Definition of analysis index

This contribution will quantitatively analyse the availability and reliability improvements from DBS under different obstructions. The employed indexes for availability and reliability analysis are defined as follows.

The availability analysis index is defined as the percentage of usable epochs for which the dilution of precision (DOP) is smaller than a given threshold:

$$Availability = \frac{\#\text{ epochs for which DOP smaller than thershold}}{\#\text{ total epochs}} \tag{6}$$

where the DOP value can be computed from the position of receiver and satellites without any real observations.

The reliability reflects the strength of mathematics model to resist bias. The minimal detected bias (MDB) is a very important indicator to reflect the reliability capability [10–13]. It is the minimal bias that the mathematical model can detect with a given test power.

Please cite this article as: S. Huang et al., Contribution of the BDS to availability and reliability improvement: A case study of dam surface displacement monitoring in China, Geodesy and Geodynamics, https://doi.org/10.1016/j.geog.2019.02.001

Assuming there is bias, called ∇_i, at the i-th observation. This bias is detected by hypothesis testing with a null and alternative hypothesis as:

$$\begin{cases} H_0: E(\boldsymbol{y}) = \boldsymbol{Ax} & \text{with } D(\boldsymbol{y}) = \boldsymbol{Q_y} \\ H_a: E(\boldsymbol{y}) = \boldsymbol{Ax} + \boldsymbol{c}_i\nabla_i & \text{with } D(\boldsymbol{y}) = \boldsymbol{Q_y} \end{cases} \tag{7}$$

where $\boldsymbol{c}_i$ is the vector with all elements being zeros except the i-th one which equals 1.

The uniformly most powerful test statistic for testing H_0 and H_a is given by:

$$T = \frac{\left(\boldsymbol{c}_i^{\mathrm{T}}\boldsymbol{Q}_{\boldsymbol{y}}^{-1}\boldsymbol{P}_{\boldsymbol{A}}^{\perp}\boldsymbol{y}\right)^2}{\boldsymbol{c}_i^{\mathrm{T}}\boldsymbol{Q}_{\boldsymbol{y}}^{-1}\boldsymbol{P}_{\boldsymbol{A}}^{\perp}\boldsymbol{c}_i} \tag{8}$$

where $\boldsymbol{P}_{\boldsymbol{A}}^{\perp} = \boldsymbol{I} - \boldsymbol{P}_{\boldsymbol{A}}$, with $\boldsymbol{P}_{\boldsymbol{A}} = \boldsymbol{A}(\boldsymbol{A}^{\mathrm{T}}\boldsymbol{Q}_{\boldsymbol{y}}^{-1}\boldsymbol{A})^{-1}\boldsymbol{A}^{\mathrm{T}}\boldsymbol{Q}_{\boldsymbol{y}}^{-1}$, is the least-squares projector matrix. The i-th diagonal element of the projector matrix is the redundancy condition of the i-th observation.

The test statistic T follows the Chi-squared distribution under H_0 and H_a, respectively:

$$T \sim \begin{cases} X^2(1,0) & \text{under } H_0 \\ X^2(1,\lambda) & \text{under } H_a \end{cases} \tag{9}$$

with the non-centrality parameter: $\lambda = \nabla_i^2\boldsymbol{c}_i^{\mathrm{T}}\boldsymbol{Q}_{\boldsymbol{y}}^{-1}\boldsymbol{P}_{\boldsymbol{A}}^{\perp}\boldsymbol{c}_i$, which can be computed given the significance level α (the probability of type *I* error) and the detection power γ ($\gamma = 1 - \beta$ with β is the chosen probability of type *II* error) [11]. With α_0 and β_0 being the chosen significance level and detection power, λ_0 follows:

$$\chi^2_{\alpha_0}(1,0) = \chi^2_{\beta_0}(1,\lambda_0) \tag{10}$$

Then MDB of the i-th observation is:

$$|\nabla_i| = \sqrt{\frac{\lambda_0}{\boldsymbol{c}_i^{\mathrm{T}}\boldsymbol{Q}_{\boldsymbol{y}}^{-1}\boldsymbol{P}_{\boldsymbol{A}}^{\perp}\boldsymbol{c}_i}} \tag{11}$$

in which, $\boldsymbol{c}_i^{\mathrm{T}}\boldsymbol{Q}_{\boldsymbol{y}}^{-1}\boldsymbol{P}_{\boldsymbol{A}}^{\perp}\boldsymbol{c}_i$ is the redundancy value. Obviously, a smaller MDB means that the higher reliability of the underlying model. In general, the higher observation precision and better redundancy are associated with a smaller MDB. In other words, with given test power, it is easier to detect the smaller gross error if its corresponding observation is more precise and the corresponding redundancy are larger.

3. Experiments and analysis

3.1. Shielding situation simulation method

An illustration of high shielding situation for dam is shown in Fig. 1. Visualizing this obstruction and satellites in the horizontal plane, the blocking scenario is shown in Fig. 2. Satellites in the obstruction shadow (called *Block Area* in Fig. 2) will be blocked. In order to investigate the contribution of BDS, different parameters of obstructions will be simulated.

The elevation e_m^i and azimuth α_m^i of satellite are calculated from its position and the receiver position. The satellite will be blocked when its elevation and azimuth satisfy condition:

$$e_m^i < arctan\left(\frac{h}{d\sqrt{1+\tan^2\left(\alpha_m^i - \alpha_0\right)}}\right) \text{ with } \alpha_0 - \beta_1 < \alpha_m^i < \alpha_0 + \beta_2 \tag{12}$$

where, $\beta_1 = acr\tan(d/l_1)$ and $\beta_2 = acr\tan(d/l_2)$.

3.2. The first experiment

In order to investigate the contribution of BDS to the availability and reliability of the BDS + GPS system, 5 different scenarios are designed (as Table 1 shown). First, the dam is simulated with the same size as the one of Sanxia dam cross the Yangtze River in Hubei Province. The simulated position taken in this analysis is SHAO (an IGS station in Shanghai) (Table 2).

In scenarios 2–5, different changing parameters of this dam, such as α_0, h, d, l_1 and l_2 ($l_1 = l_2$), are specified in given location. For each scenario, the availability and reliability are analyzed by using data with 30 seconds sampling interval in No.216 day of 2016 year.

In order to show the blocking effect of dam, the availability of using data is analyzed firstly when there is not obstruction. The number of visible satellites changes between 15 and 23, of which BDS changes from 8 to 12. The PDOP is smaller than 6 over the whole day for neither GPS-only or BDS-only. In other words, both systems can positioning independently when there is not obstruction. The improvement of the combined systems is obvious: the number of visible satellites is almost doubled compared to each single system, and the PDOP is reduced about 50%. The same analysis is processed in scenario 1, the results are shown in Fig. 3. It can be seen that obstruction has an obvious impact on the availability of positioning: about 70% epochs cannot position when

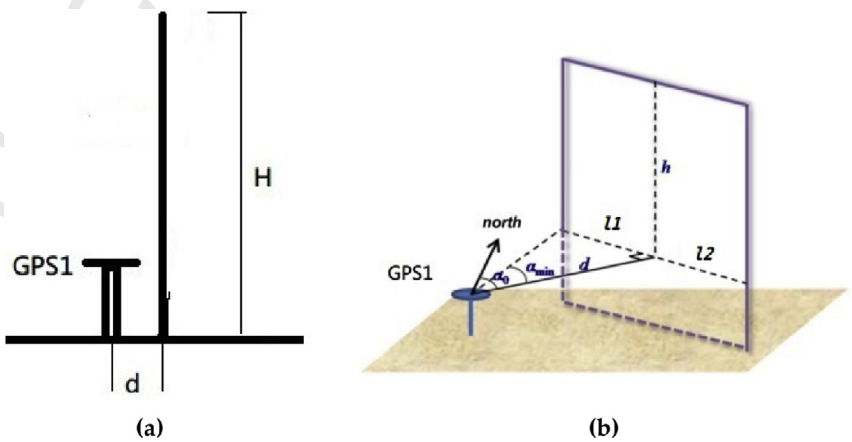

Fig. 1. The geometric relationship between the receiver with obstruction. Left one is plat diagram, while right one 3D diagram. H is the height of obstruction, d is the distance between receiver with obstruction, l1 and l2 denote the size of obstruction, and α_0 is it's direction.

Please cite this article as: S. Huang et al., Contribution of the BDS to availability and reliability improvement: A case study of dam surface displacement monitoring in China, Geodesy and Geodynamics, https://doi.org/10.1016/j.geog.2019.02.001

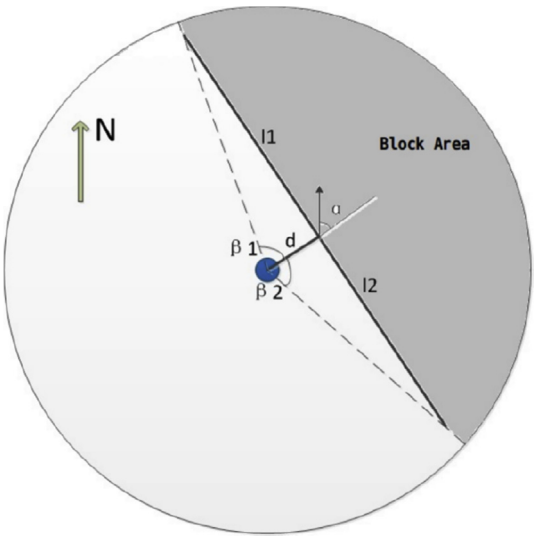

Fig. 2. The shadow of the dam in the station plate coordination of station.

Table 1
All simulation scenarios in the first experiment.

Scenario	d [m]	$l_1 = l_2$ [m]	h [m]	α_0 [°]
1	1.0	1550	185	30
2	1.0	1550	185	0:10:360
3	1.0	1550	100:20:200	30
4	1.0	500:500:2000	185	30
5	1.0, 10:10:200	1550	185	30

'a:b:c' denotes that the value changes from 'a' to 'c' in step 'b'.

Table 2
All simulation scenarios of experiment 2.

Scenario	station location	d [m]	$l_1 = l_2$ [m]	h [m]	α_0 [°]
6	latitude: N 0° ~ 54° longitude: E 70° ~ 135°	1.0	1550	185	0
7	Same as scenario 6	1.0	1550	185	90
8	Same as scenario 6	1.0	1550	185	180

there is only GPS because the number of visible satellites is less than 4 or PDOP > 6. Unusable epoch rate of BDS, on the other hand, is only about 10%. The reason is that the GEO satellites cannot be shielded due to the dam is in the north of receiver. The availability of combined systems can reach 100%, but the PDOP is always larger than the one of case without obstructions.

The contribution of BDS to the MDB reduction is also analyzed (all MDB analysis uses $\alpha = 5\%$ and $\beta = 80\%$). GPS 20 satellite code and phase data' MDB values of alone/combined systems are shown in Fig. 4. For pseudorange, the MDB value of the combined systems is equal to the value of the independent system since the accuracy of pseudorange is much lower than that of phase observable. The result of redundancy condition (both equal 1) show the same conclusion. For phase observable, the MDB value of combined systems are all smaller than that of GPS-only system. The result of redundancy condition also shows that the redundancy condition of combined systems is bigger and smoother. Otherwise, the change of MDB value is inversely proportional to the elevation angle since the weight of ZD phase observable is inversely proportional to it too. A similar analysis is done for the BDS satellites. For pseudorange, there is no difference between alone and combined systems. Therefore, the following MDB value analysis in this paper will only focus on the phase observable (Fig. 5).

Comparing with BDS-only system, the MDB value of BDS satellites is smaller in combined systems. However, the reduction is not obvious as that for GPS. In other words, the contribution of combined systems for BDS MDB decrease is more obvious than that for GPS. In order to show the average improvement, the MDB mean value of whole day is counted for each satellites in the single and combined systems (shown as Fig. 6). This result proves the previous conclusion.

The direction of dam is changed in scenario 2. The mean values (PDOP and availability) for dams in each direction are analyzed in order to show the relationship between availability and the direction of dam (shown in Fig. 7). For single system, the average PDOP is almost bigger than the threshold, thus both GPS and BDS cannot monitor the deformation of dam alone. This can be proved by availability results for the whole day too (shown in Fig. 7(b)). The availability of BDS + GPS is obviously higher than the one for each system alone. For each direction, the MDB average for each satellite is shown in Fig. 8. The value of combined systems is obviously smaller than that of each system alone. In other words, the ability to detect biases in the combined systems is stronger than that each system alone. Otherwise, the similar phenomenon can be seen

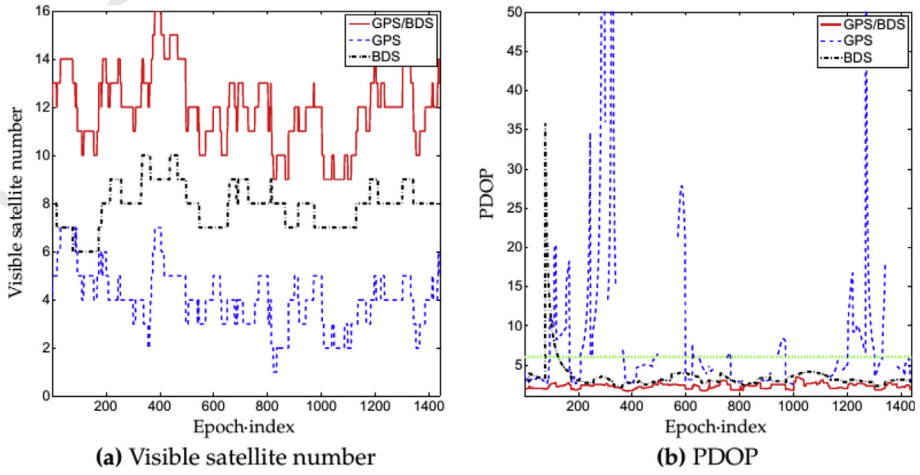

Fig. 3. visible satellite number and PDOP analysis result in the scenario 1.

Please cite this article as: S. Huang et al., Contribution of the BDS to availability and reliability improvement: A case study of dam surface displacement monitoring in China, Geodesy and Geodynamics, https://doi.org/10.1016/j.geog.2019.02.001

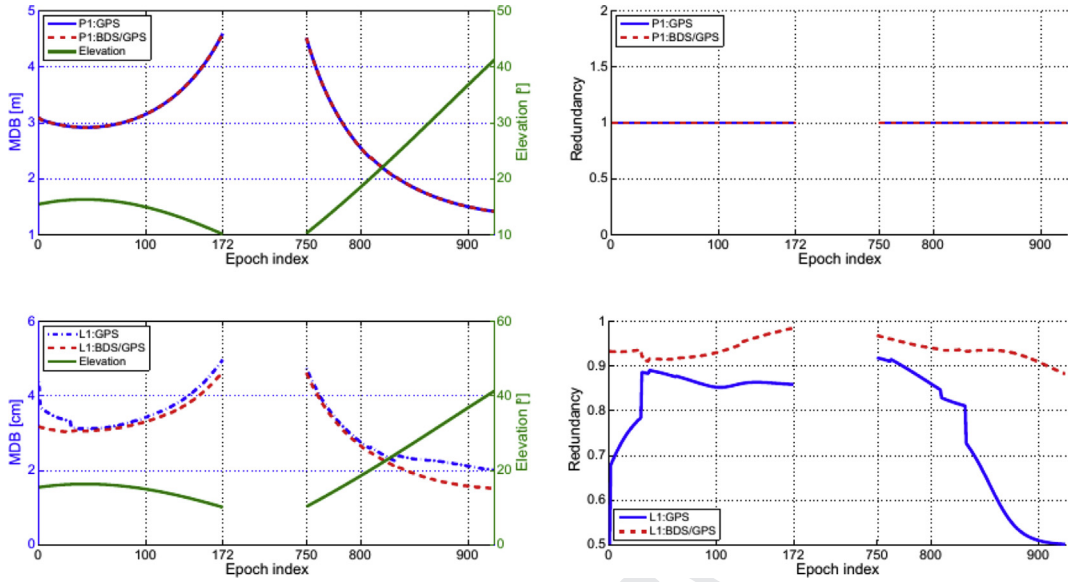

Fig. 4. The MDB of GPS 20 satellite in alone/combined systems. The ticks on the X axes are split due to the not-continue visible period of the MEO satellite. The upper row is the result for the code observable; while the lower is for the one of phase observable.

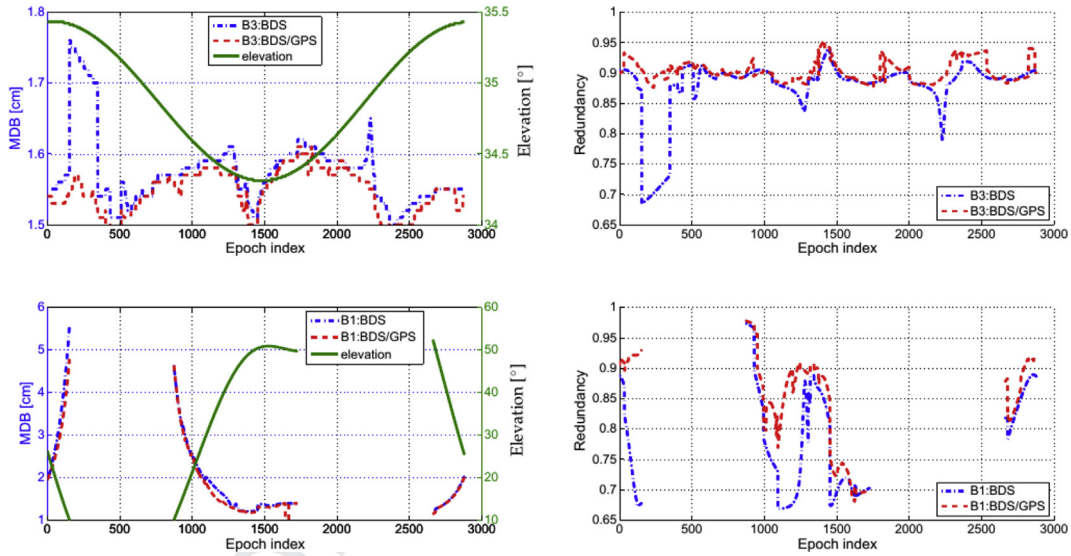

Fig. 5. MDB of BDS satellite in alone/combined systems. The upper row is the result of PRN 1 BDS satellite (GEO) in 'B3' frequency; while under the one of PRN 9 BDS satellite (IGSO) in 'B1' frequency.

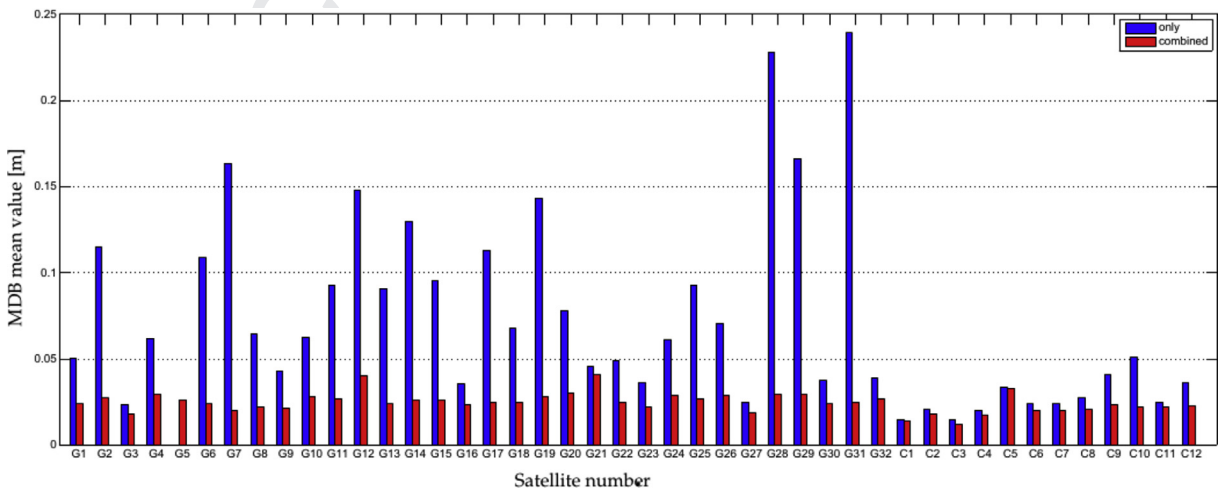

Fig. 6. MDB mean value of whole day for each satellite in scenario 1.

Please cite this article as: S. Huang et al., Contribution of the BDS to availability and reliability improvement: A case study of dam surface displacement monitoring in China, Geodesy and Geodynamics, https://doi.org/10.1016/j.geog.2019.02.001

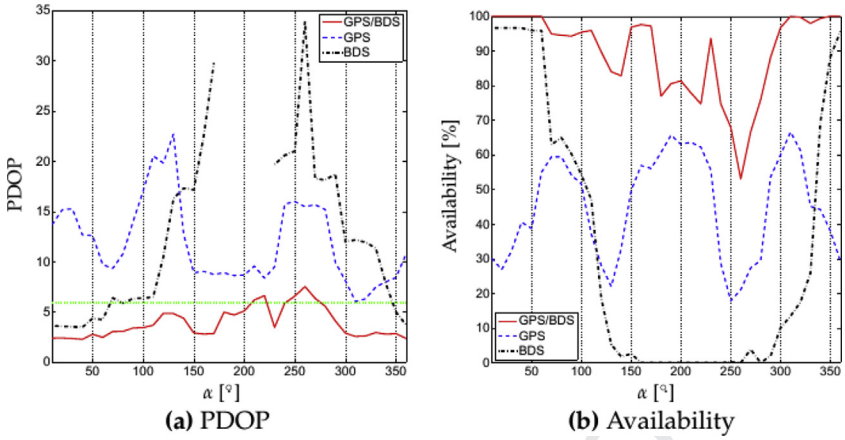

(a) PDOP (b) Availability

Fig. 7. PDOP and availability average in every directions scenario 2.

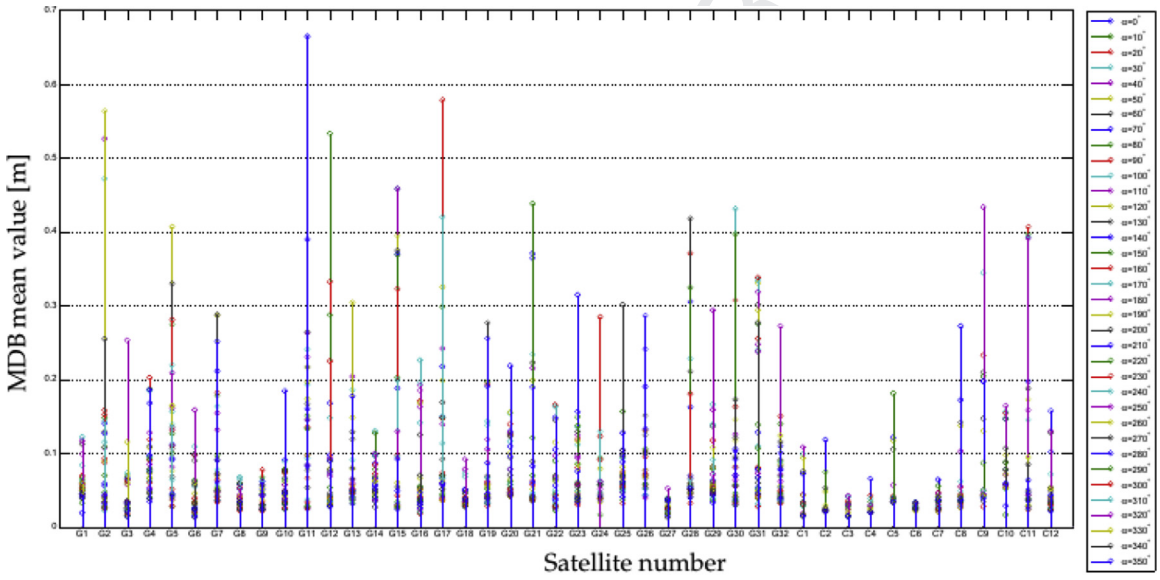

(a) Alone system

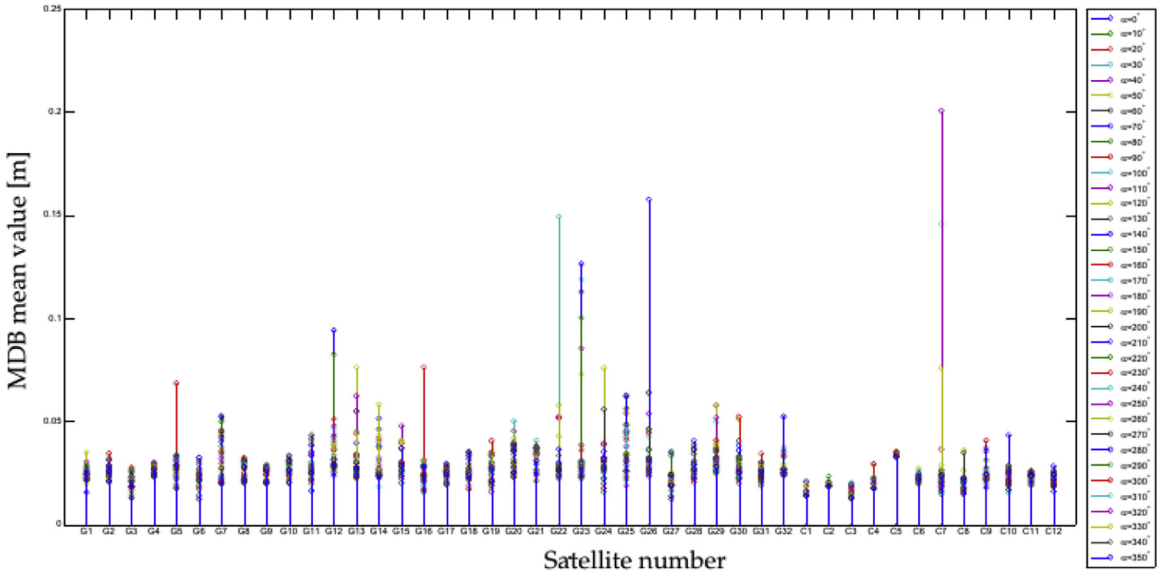

(b) Combined system

Fig. 8. MDB mean value of each satellite for every directions scenario 2.

Please cite this article as: S. Huang et al., Contribution of the BDS to availability and reliability improvement: A case study of dam surface displacement monitoring in China, Geodesy and Geodynamics, https://doi.org/10.1016/j.geog.2019.02.001

from the MDB mean value analysis: the decrease for GPS is bigger than the one for BDS.

Between scenario 3 and 5, the experiment simulated the obstacles of different size. Meanwhile, the distance from these dam to receiver were changed. Fig. 9 shows the effect of size change to availability in different distances away from receiver. The number of visible satellites and PDOP are not changing according with the change of size when the dam is very close to receiver, such as $d = 1$ m (shown in Fig. 9(a) and (d)) and $d = 10$ m (shown in Fig. 9(b) and (e)), because even a small obstruction can block a large part of the sky. The effect of obstruction on availability decreases systematically when it is away from receiver, until the distance is far enough to cause no obstruction. Fig. 10 focuses on a specific size in order to show the variation of number of visible satellites and PDOP according with increasing distance. The number of visible satellites as a function of the distance away from the receiver changes in the form of logarithmic function curve; while the PDOP value in the form of exponential function curve.

3.3. The second experiment

In order to analyse the contribution situation in different locations, the second experiment fixes the obstruction parameters, $d = 1$ m, $l_1 = l_2 = 1550$ m, $h = 185$ m and $\alpha_0 = 0$. Then, similar simulations were performed in specific ranges (latitude from 0° to N54° and longitude E70° to E135°). This is referred to as scenario 6. The scenarios 7 and 8 are similar to scenario 6 but with different obstruction azimuths $\alpha_0 = 90$ and $\alpha_0 = 180$, respectively.

Between scenarios 6 and 8, simulation settings are similar except for the azimuth of the obstruction. The percentages of usable epochs for GPS-only and BDS + GPS are shown in Fig. 11. In scenario 6, availability is generally smaller than 50% over most of the area. Moreover, the availability for different scenarios are similar.

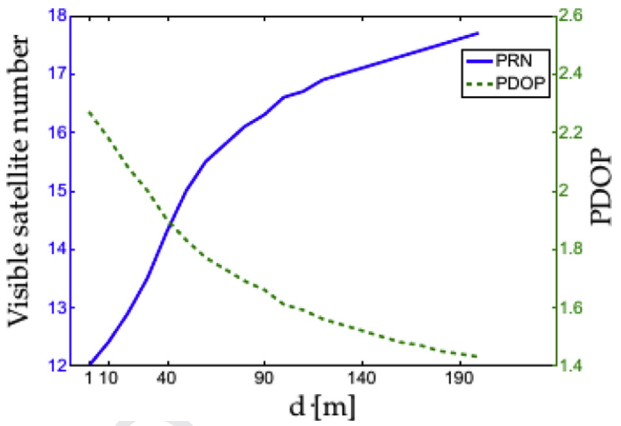

Fig. 10. Change of visible satellite number and PDOP mean values according with the distance of dam away from receiver (h = 110 m, l = 1100 m) between scenarios 3 and 5.

BDS + GPS, on the other hand, is available in most of the region. In addition, we can see that the availability changes with the direction of the dam as follows:

(1) In scenario 6, the dam is in north of the receiver. The improvement of combined BDS is the most obvious one of improvements in all scenarios.
(2) In scenario 7, the availability of GPS + BDS is obviously divided by two longitude lines since the dam is north-south. All GEO satellites are blocked when the dam is located in the west of E80°; 3 or 4 GEO satellites are blocked by the dam when it located between E80° and E100°; almost all GEO satellites can be tracked when the dam is located in east of E100°.
(3) In scenario 8, the availability of combined systems is divided by one latitude line since the dam is west-east. When the

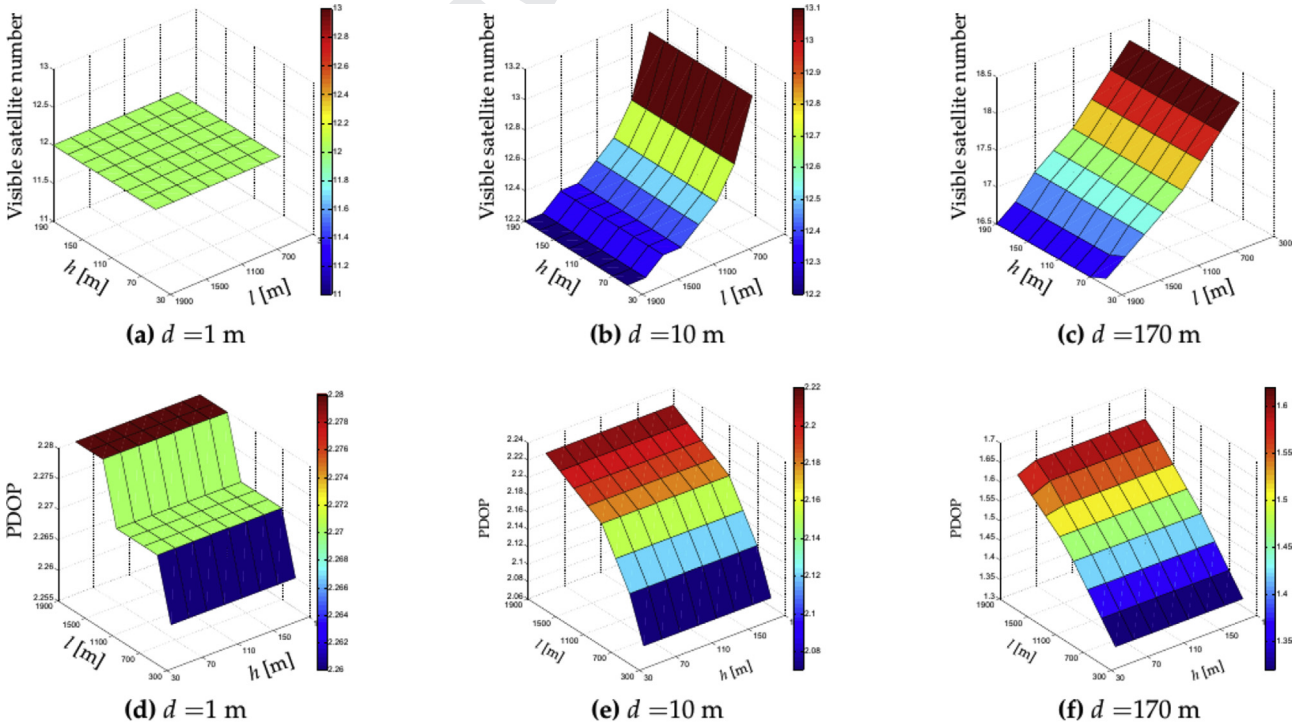

Fig. 9. Visible satellite number the whole day mean values between scenarios 3 and 5.

Please cite this article as: S. Huang et al., Contribution of the BDS to availability and reliability improvement: A case study of dam surface displacement monitoring in China, Geodesy and Geodynamics, https://doi.org/10.1016/j.geog.2019.02.001

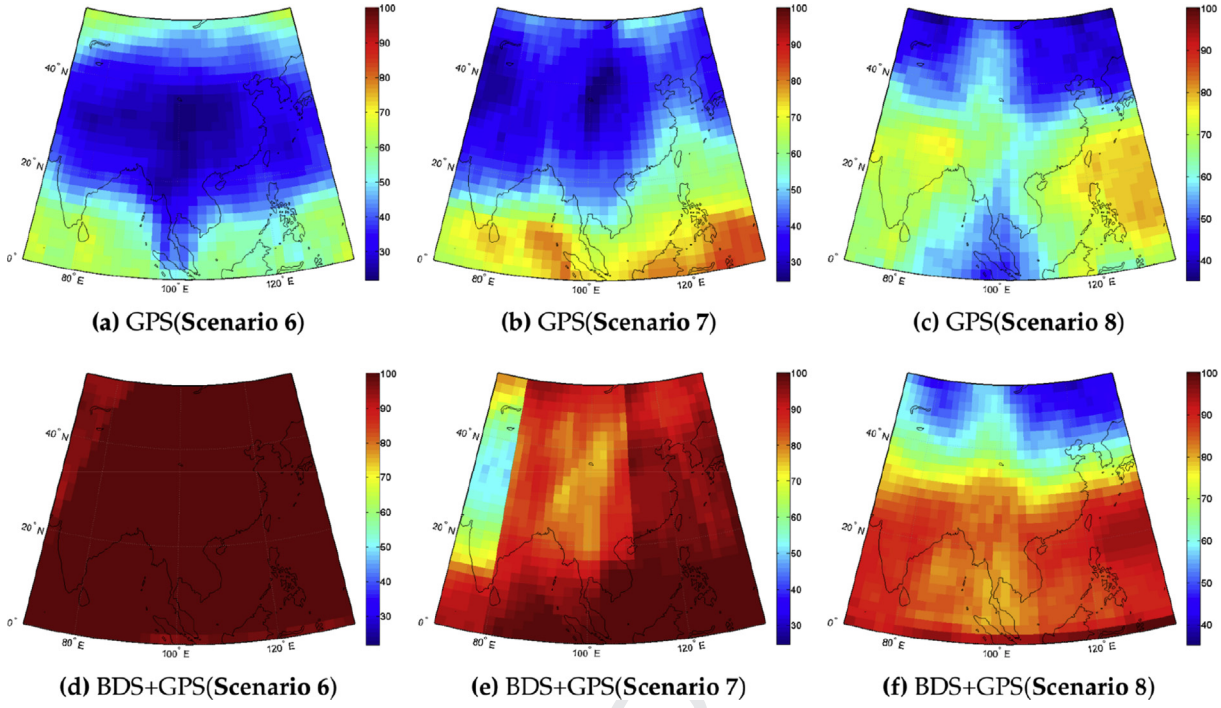

Fig. 11. The availability analysis results between scenario 6 and 8 [%].

dam is located in the north of N35°, most GEO satellites are obscured.

Because the reliability of GPS satellite is improved obviously in the combined systems, the average MDB analysis only uses all GPS satellites and excludes BDS satellites. The results of all scenarios are shown in Fig. 12. In all scenarios, the MDB average value of combined systems is smaller than that of GPS-only system. The reliability improvement in scenario 8 is the most obvious one of the three scenarios. Interestingly, scenario 8 is the worst case for single-system reliability due to the shielding of many satellites. This proves the conclusion again that the worse the performance of

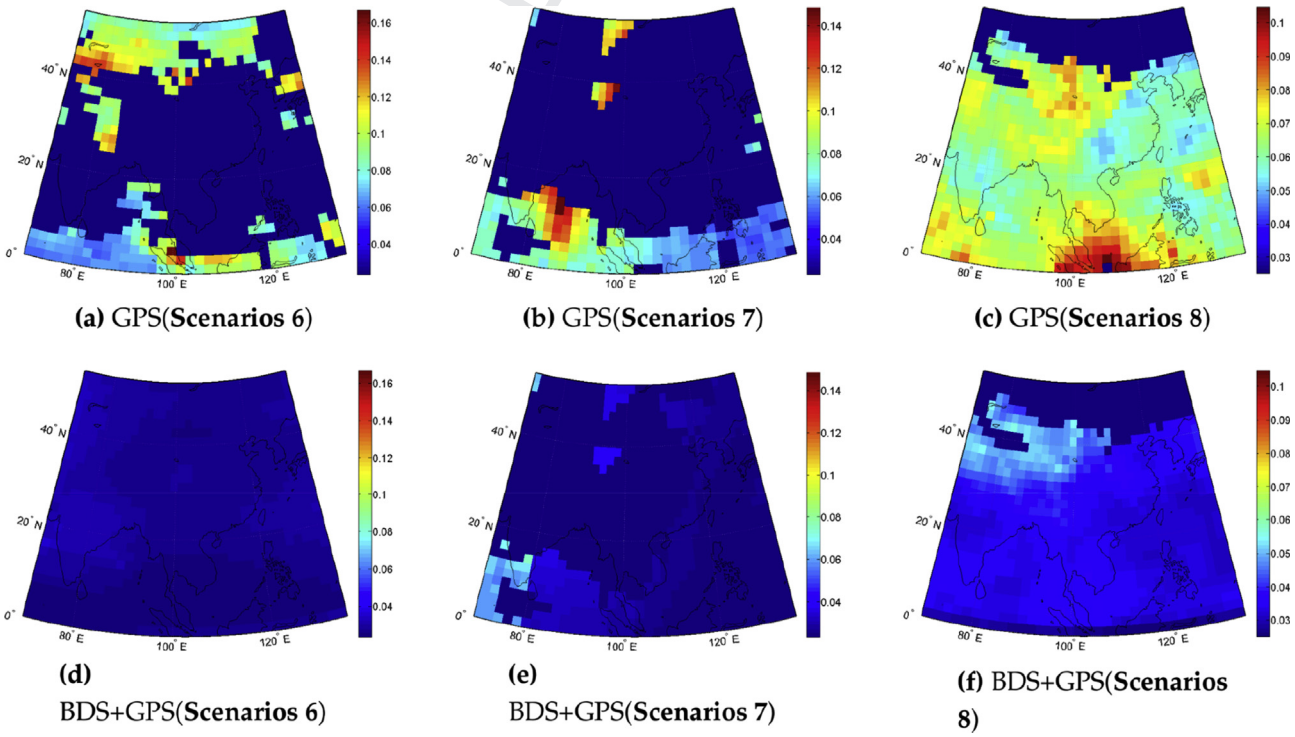

Fig. 12. Average MDB of all GPS satellites between scenario 6 and 8 [m].

Please cite this article as: S. Huang et al., Contribution of the BDS to availability and reliability improvement: A case study of dam surface displacement monitoring in China, Geodesy and Geodynamics, https://doi.org/10.1016/j.geog.2019.02.001

independent systems, the greater the improvement in availability and reliability of combined systems.

4. Conclusions

Availability and reliability are the important evaluation indicators of GNSS deformation monitoring system. A BDS + GPS deformation monitoring system has better availability and reliability than a GPS-only system, especially in high shielding situations. In this contribution, we chose the number of visible satellites and PDOP to analyse the availability, and MDB to analyse the reliability. Many obstruction scenarios are simulated in order to demonstrate the contribution to availability and reliability of BDS to the BDS + GPS deformation monitoring system. The data required for this simulation method is just the position of receiver and the ephemeris in the analysis period. The results show that the current BDS constellation could improve the availability of deformation monitoring significantly, when GEO satellites are not blocked. In addition, the contribution of BDS to deformation monitoring varies in different places due to the different number of visible GEO/IGSO satellites. Adding the BDS system to GPS can also reduce the MDB of the total system. The MDB contribution for phase observations is more obvious than the one for the code observable because of the much higher precision of the phase measurement. The improvement of MDB also depends on the blocking situation of the GEO satellites. In summary, the combination of BDS and GPS can improve the availability and reliability of the whole system. In addition, the improvement of the combined systems in availability and reliability will be obvious when the obstruction does not shield all GEO satellites.

Conflicts of interest statement

The authors are very much thankful to three anonymous reviewers and Professor LI Bofeng from The Tongji University, Shanghai, China for their valuable comments, which are considered helpful to improve the manuscript significantly. In addition, the authors acknowledge that, this work is supported by the basic ability promotion project for young and middle-aged teachers from the Guangxi Education Department (2017KY0029). Except, The Guangxi University, Shanghai Astronomical Observatory, China Academy of Sciences has involved in this work. The manuscript prepared is the sole work of the authors mentioned in the manuscript.

Acknowledgements

This work is supported by the basic ability promotion project for young and middle-aged teachers from the Guangxi Education Department (2017KY0029). Three anonymous reviewers and the responsible editor, Professor LI Bofeng, are appreciated for their valuable comments, which are considered helpful to improve the manuscript significantly.

References

[1] J.A. Behr, K.W. Hudnut, N.E. King, Monitoring structural deformation at Pacoima dam, California using continuous GPS, Seismol Res. Lett. 69 (1998).
[2] M. Battaglia, P. Segall, J. Murray, P. Cervelli, J. Langbein, The mechanics of unrest at Long Valley caldera, California: 1. Modeling the geometry of the source using GPS, leveling and two-color EDM data, J. Volcanol. Geotherm. Res. 127 (2003) 195–217.
[3] M. Battaglia, P. Segall, C. Roberts, The mechanics of unrest at Long Valley caldera, California. 2. Constraining the nature of the source using geodetic and micro-gravity data, J. Volcanol. Geotherm. Res. 127 (2003) 219–245.
[4] M. Alba, L. Fregonese, F. Prandi, M. Scaioni, P. Valgoi, Structural Monitoring of a Large Dam by Terrestrial Laser Scanning, International Archives of Photogrammetry, Remote Sensing and Spatial Information Sciences, 2006.
[5] D. Gonzalez Aguilera, J. Gomez Lahoz, J. Sanchez, A new approach for structural monitoring of large dams with a three-dimensional laser scanner, Sensors 8 (2008) 5866–5883.
[6] M. Alba, G. Bernardini, A. Giussani, P.P. Ricci, F. Roncoroni, M. Scaioni, P. Valgoi, K. Zhang, Measurement of dam deformations by terrestrial interferometric techniques, Int. Arch. Photogramm. Remote Sens. Spat. Inf. Sci. 1374 (2008) 133–139.
[7] Y. Yang, J. Li, J. Xu, J. Tang, H. Guo, Contribution of the Compass satellite navigation system to global PNT users, Sci. Bull. 56 (2011) 2813–2819.
[8] B. Li, Y. Shen, X. Zhang, Three-frequency GNSS navigation prospect demonstrated with semi-simulated data, Adv. Space Res. 51 (2013) 1175–1185.
[9] B. Li, Y. Shen, Y. Feng, W. Gao, L. Yang, GNSS ambiguity resolution with controllable failure rate for long baseline network RTK, J. Geod. 88 (2014) 99–112.
[10] P.J.G. Teunissen, Quality control in integrated navigation systems, IEEE Aerosp. Electron. Syst. Mag. 5 (1990) 35–41.
[11] P.J.G. Teunissen, Minimal detectable biases of GPS data, J. Geod. 72 (1998) 236–244.
[12] P.J.G. Teunissen, P. Joosten, D. Odijk, The reliability of GPS ambiguity resolution, GPS Solut. 2 (1999) 63–69.
[13] P.J.G. Teunissen, D. Odijk, C.D.D. Jong, Ambiguity Dilution of Precision: An Additional Tool for GPS Quality Control, vol. 21, LGR-Series Delft Geodetic Computing Centre, Delft, 2000, pp. 261–270.

Dr. Shanqi Huang: He obtained Ph.D. degree from Tongji University in 2015 with dissertation focusing on the deformation monitoring with GNSS. He works at the Guangxi University since June 2015.

Prof. Dr. Junping Chen: He is a professor at Shanghai Astronomical Observatory (SHAO), Chinese Academy of Sciences, and head of the GNSS Analysis Center at SHAO. His current research activities focus on real-time GNSS applications, Multi-GNSS analysis, precise orbit determination, and satellite-based GNSS augmentation systems.

Dr. Hu Wang: He obtained Ph.D. degree from Tongji University in 2007 with dissertation focusing on the GNSS data processing. He works at the Chinese Academy of Surveying & Mapping.